International Journal of Thermophysics, Vol. 15, No. 6, 1994

Dynamics of Crossover from Diffusion Growth to Coarsening in Quenched Binary Mixtures[1]

M. Tokuyama[2,4] and Y. Enomoto[5]

The effect of a high volume fraction on the dynamics of phase separations in off-critically quenched binary mixtures, such as binary alloys and polymer blends, is discussed from a new unifying point of view. Three characteristic stages are shown to exist after the nucleation stage. The first is the early stage [E] where the droplets grow directly and independently from the solution by diffusion. The second is the intermediate stage [I], where the growth is no longer independent due to the three kinds of interactions among droplets: the many-body interaction, the coagulation, and the Ostwald ripening. The third is the coarsening stage [C] where the growth from the solution is over. The dynamical behavior of phase separations is investigated analytically through the whole stages, including the dynamical scaling behavior, time exponents, and crossover. The numerical simulation is also performed to confirm the theoretical prediction.

KEY WORDS: coagulation; crossover; diffusive long-range interactions; dynamical scaling; finite volume fraction; Ostwald ripening; phase separations.

1. INTRODUCTION

In spite of many recent works on the dynamics of phase separations in off-critically quenched binary mixtures, including experimental [1–6], numerical [7–10], and theoretical [11–14] approaches, there is still a poor theoretical understanding of the crossover phenomena from earlier times to later times. In a previous paper [15], we presented the systematic theory

[1] Paper presented at the Twelfth Symposium on Thermophysical Properties, June 19–24, 1994, Boulder, Colorado, U.S.A.

[2] Department of Chemistry, Massachusetts Institute of Technology, Cambridge, Massachusetts 02139, U.S.A.

[3] Present address: Statistical Physics Division, Tohwa Institute for Science, Tohwa University, Fukuoka 815, Japan.

[4] To whom correspondence should be addressed.

[5] Department of Physics, Nagoya Institute of Technology, Nagoya 466, Japan.

0195-928X/94/1100-1145$07.00/0

for the crossover phenomena, which enables us to describe not only the time evolution of the single-droplet size distribution function but also that of the structure function. Thus, we have shown that this theory yields a good description of the dynamics of phase separations in off-critically quenched binary systems having a low volume fraction of one phase 0.1 [15–17]. Beyond this volume fraction, however, the encounters of the droplets, in which two or more droplets meet within a distance less than their mean linear dimension, also become important. In this paper, therefore, we discuss the extension of the previous theory to the case of higher volume fractions and also perform the computer simulation to confirm the theoretical prediction.

When the binary system is off-critically quenched into the two-phase region from the one-phase region, it undergoes phase separation by nucleation and growth of droplets of the minority phase. There are three kinds of growth mechanisms which cause droplets growth after the nucleation stage. The first is a direct growth mechanism where the droplets grow directly from the supersaturated solution by diffusion. This mechanism does not change the number of droplets but increases the volume fraction. The second mechanism is the Ostwald ripening mechanism, where the larger droplets grow at the expense of the smaller droplets [18]. This drastically reduces the number of droplets but does not change the volume fraction. The third mechanism is the coagulation mechanism, where when two or more droplets meet, the larger of them absorbs the smaller, conserving their total volume [18]. These mechanisms become important on different time scales, depending on the value of the volume fraction. In this paper, we restrict ourselves to the case of instantaneous nucleation where all droplets are nucleated only during the initial short time, that is, a nucleation stage. Then, there exist three characteristic growth stages after the nucleation stage. The first is an early stage [E] where the diffusive interactions among droplets are not important, and the droplets, which have reached an appreciable size, grow directly and independently from the supersaturated solution by diffusion. The number density of the droplets does not change but the volume fraction of the droplets increases rapidly. After this stage, the three kinds of growth mechanisms compete with each other. This is an intermediate stage [I] where the growth is no longer independent and is slowed down by the many-body effect. It depends on the value of the volume fraction, which mechanism first becomes important here. The final stage is a coarsening stage [C] where the growth from the solution is over and the volume fraction becomes constant.

Similarly to I, the single-droplet-size distribution function $f(R, t)$ with radius R and the structure function $S(\mathbf{k}, t)$ are shown to satisfy the dynamical scaling laws at each stage,

$$f(R, t) = \frac{n(t)}{\langle R \rangle(t)} F\left(\frac{R}{\langle R \rangle}, t\right) \tag{1}$$

$$S(\mathbf{k}, t) = k_{\mathrm{M}}(t)^{-d} \Phi(t)^{\delta} \Psi\left(\frac{\mathbf{k}}{k_{\mathrm{M}}}, t\right) \tag{2}$$

with the peak position of $S(\mathbf{k}, t)$ as a function of $\mathbf{k}$,

$$k_{\mathrm{M}}(t) \sim L(t)^{-1} \sim \Phi(t)^{1/d} / \langle R \rangle(t) \tag{3}$$

and the temporal power laws

$$\langle R \rangle(t) \sim t^{\eta_R}, \qquad n(t) \sim t^{-\eta_n}, \qquad \Phi(t) \sim t^{\eta_\Phi}, \qquad k_{\mathrm{M}}(t) \sim t^{-\eta_k} \tag{4}$$

where $n(t)$ denotes the number density of the droplets, $\langle R \rangle(t)$ the average droplet radius, $L(t) = [4\pi n(t)/3]^{-1/3}$ the interdroplet distance, and $d = 3$ here. The time exponents satisfy the relation

$$\eta_\Phi = d\eta_R - \eta_n, \qquad \eta_k = \eta_R - \eta_\Phi/d = \eta_n/d \tag{5}$$

where $\delta = 2$ for stage [E] and $\delta = 1/d$ for stages [I] and [C]. Here $\Phi(t)$ is the time-dependent volume fraction of the droplets and satisfies the conservation law

$$\Phi(t) + \Delta(t) = Q \tag{6}$$

where $\Delta(t)$ represents the supersaturation and Q the total initial supersaturation. We should mention that the scaling functions $F(x, t)$ and $\Psi(x, t)$ still depend on time over the region, where the volume fraction $\Phi(t)$ is changing in time, and then reach the time-independent functions for long times, where $\Phi(t) = Q$. In the following sections, we discuss only the time evolution of the distribution function.

2. THEORY

Here we discuss the extension of the previous theory to the case of higher volume fractions.

We consider a three-dimensional system, which consists of N spherical droplets of the minority phase with radius $R(t)$ and position-vector $\mathbf{X}_i(0)$ $(i = 1, 2, \ldots, N)$, and a supersaturated solution of the majority phase. We assume that the droplets of the minority phase are spherical even for higher volume fractions and, also, that the distribution of their positions is stationary. The system has three characteristic lengths; the average droplet radius, $\langle R \rangle(t)$; the interdroplet distance, $L(t)$ [or $k_{\mathrm{M}}(t)^{-1}$]; and the

screening length, $l(t) = [4\pi n(t)\langle R\rangle(t)]^{-1/2}$, within which droplets have correlations.

The concentration field of the supersaturated solution is described by the diffusion equation with the Gibbs–Thompson relationship as the boundary condition and the appropriate initial condition. Similarly to I, by solving the diffusion equation and using the mass conservation for each droplet, on the length scale of order l, one can derive the rate equation for the radius of the ith droplet,

$$\frac{dR_i(t)}{dt} = \frac{\alpha D}{R_i(t)^2}\left[\frac{R_i(t)}{R_C(\mathbf{X}_i, t)} - 1\right] + \left(\frac{dR_i}{dt}\right)_E \tag{7}$$

with the critical radius

$$R_C(\mathbf{X}_i, t) = \alpha \Bigg/ \left[Q - \sum_{j(\neq i)}^{N} \int_0^t ds \frac{\exp[-|\mathbf{X}_i - \mathbf{X}_j|^2/4D(t-s)]}{[4\pi D(t-s)]^{3/2}} \frac{d}{ds} \times \left(\frac{4\pi}{3} R_j(s)^3\right)\right] \tag{8}$$

where α is the capillary length, and D the diffusion coefficient. Equation (7) is also supplemented by the conservation of mass for the entire system, which is given by Eq. (6). The first term in Eq. (7) represents the diffusion current of solute across the boundary of the ith droplet. The second term, $(dR_i/dt)_E$, represents the encounter term, which one can deal with numerically only by computer simulations since its explicit form is not known yet at the microscopic level.

Equation (7) is a starting non-Markov equation for studying the phase-ordering dynamics in the metastable system over the whole time region after the nucleation stage. The first term of the denominator of Eq. (8) is a single-body effect of order Φ^0. The second term represents a many-body effect due to the diffusive long-range interactions among droplets separated by a distance of order l and contains the higher-order terms in $\Phi^{1/2}$. Because of the many-body effect and the encounter effect, one can solve Eq. (7) only numerically by computer simulations. As was shown in I, therefore, we must further reduce it to obtain two kinds of macroscopic equations which we can reasonably analyze. One is a kinetic equation for the single-droplet-size distribution function $f(R, t)$ with radius R, which is measured by an electron microscope. The other is a linear equation for the dynamic structure function $S(\mathbf{k}, t)$, which is observable by using small-angle scattering of neutrons, X-rays, or light. Next we discuss only the kinetic equation.

Define the dimensionless time τ and radius a by $\tau = \alpha D t/R_0^3$, $a = R/R_0$, where $R_0 = \alpha/Q$ denotes the initial critical radius. Starting from Eq. (7), one can then obtain the non-Markov kinetic equation, up to order Φ,

$$\frac{\partial}{\partial \tau} f(a, \tau) = \frac{1}{\langle a \rangle^3} \frac{\partial}{\partial \rho} \frac{1}{\rho^2} \left[\dot{\lambda} + \varepsilon v^{(1)} + \varepsilon^2 v^{(2)} + \varepsilon \left\{ -\rho \left(\dot{\lambda} - \frac{\langle \dot{\lambda} \rangle}{\beta} \right) + \frac{\langle \dot{\lambda}^2 \rangle}{\beta \mu_{-1}} \rho \frac{\partial}{\partial \rho} \frac{1}{\rho} \right\} \right] f(R, t) + \left(\frac{\partial f}{\partial \tau} \right)_E \tag{9}$$

with the screening terms

$$\begin{aligned} \dot{\lambda}(\tau) &= 1 - \beta(\tau)\, \rho \\ \beta(\tau) &= \langle a \rangle(\tau) \left[1 + 3 \int_0^{\tau - \tau_S} \langle \dot{\lambda} \rangle(\tau_S, y)\, v(\tau_S, y)\, dy \right] \\ v^{(1)}(\tau) &= \rho(\dot{\lambda} - \langle \rho \dot{\lambda} \rangle) \\ v^{(2)}(\tau) &= \tfrac{1}{2} \mu_2 v^{(1)}(\tau) + \rho(\rho \dot{\lambda} - \langle \rho^2 \dot{\lambda} \rangle) + \rho(b\rho \dot{\lambda} - \langle b \rho^2 \dot{\lambda} \rangle) \\ &\quad - \rho(\rho^2 - \mu_3) \langle \rho^2 \dot{\lambda}/(1 - \rho) \rangle + \rho(\rho - \mu_2) \langle \rho \dot{\lambda} \rangle (\gamma_E + \ln 6 + \tfrac{1}{2} \ln \varepsilon) \end{aligned} \tag{10}$$

where $\varepsilon(\tau) = [3\Phi(\tau)/\mu_3(\tau)]^{1/2}$, $\Phi(\tau) = (Q/\tau_3)\, v(\tau) \langle a^3 \rangle(\tau)$, $\rho = R/\langle R \rangle = a/\langle a \rangle$, $\mu_n(\tau) = \langle \rho^n \rangle(\tau)$, $v(\tau) = n(\tau)/n(0)$, $b(\rho') = \langle \rho^2/(1 - \rho\rho') \rangle$, and γ_E the Euler's constant. Here $\tau_S = Q \langle a \rangle(0)^3/\Phi(0)$ is the screening time over which the diffusive long-range interactions become important, where the brackets denote the average over the relative-droplet-size distribution function $F(\rho, \tau)$. Here there are two kinds of many-body effects due to the diffusive long-range interactions; a static many-body (screening) effect, which is determined only by the distribution function $F(\rho, \tau)$, and a dynamic many-body (correlation) effect, which is determined by the correlation functions. The terms, $\dot{\lambda}(\tau)$, $v^{(1)}(\tau)$, and $v^{(2)}(\tau)$ represent the screening effects of order Φ^0, $\Phi^{1/2}$, and Φ, respectively. The last term in the square brackets in Eq. (9) gives the correlation effect of order $\Phi^{1/2}$, where the terms of order Φ are omitted for simplicity.

The second term of Eq. (9), $(\partial f/\partial \tau)_E$, represents the encounter effect. Under the binary encounter approximation, one can write it as [18]

$$\left(\frac{\partial f}{\partial \tau} \right)_E = \frac{1}{\tau_E} \left[\frac{1}{2} \int_0^{V} dV'\, w(\rho^3 - \rho'^3, \rho'^3, \tau)\, g(V - V', \tau)\, f(a', \tau) - f(a, \tau) \int_0^{\infty} dV'\, w(\rho^3, \rho'^3, \tau)\, g(V', \tau) \right] \tag{11}$$

where $V=R^3$, $f(a,\tau)=3R^2g(R^3,\tau)$, and $\tau_E=(\tau_S/16Q)^2/2$ is the characteristic time for encounters. Here $w(\rho^3,\rho'^3,\tau)$ denotes the encounter frequency. For long time this reduces to $w(\rho^3,\rho'^3,\tau)\sim(\rho^3+\rho'^3)/2n(0)$ [18].

Equation (9) is a kinetic equation which describes the causal motion of the droplet growth over whole stages. From this equation, the distribution function $f(a,\tau)$ is then shown to satisfy the dynamical scaling given by Eq. (1). From Eq. (9) we also find the growth laws

$$\begin{aligned}\frac{d}{d\tau}\langle a^3\rangle(\tau)&=\mu_3(\tau)\,K_0(\tau)-3\langle\lambda\rangle(\tau)+(\tau_S/Q)\,\sigma(\tau)\,\Phi(\tau)\\ \frac{d}{d\tau}\ln n(\tau)&=-\frac{K_0(\tau)}{\langle a\rangle(\tau)^3}-\sigma(\tau)\,v(\tau)\end{aligned}\tag{12}$$

with the coarsening rate

$$K_0(\tau)=\lim_{\rho\to 0}F(\rho,\tau)/\rho^2\tag{13}$$

where

$$\sigma(\tau)=\frac{n(0)}{2\tau_E}\int_0^\infty d\rho\int_0^\infty d\rho'\,w(\rho^3,\rho'^3,\tau)\,F(\rho,\tau)\,F(\rho',\tau)\tag{14}$$

As is seen from Eqs. (12), there are three kinds of growth mechanisms. The first is the direct growth mechanism from the supersaturated solution which is described by the term $\langle\lambda\rangle$, where $\langle\lambda\rangle\sim-\langle a\rangle$ for the single-body effect when $\tau<\tau_S$, and $\langle\lambda\rangle\sim-\langle a\rangle^{-1}$ for the many-body effect when $\tau\geqslant\tau_S$. The second is the Ostwald ripening mechanism which is described by the term $K_0(\tau)$. The third is the encounter mechanism which is described by the term $\sigma\Phi$. After the nucleation stage, therefore, there exist three characteristic stages: the early stage [E], the intermediate stage [I], and the coarsening stage [C]. Depending on the value of the volume fraction Q, we have the following three cases. The first is the case [1] $Q<Q_0$ with $\tau_S<\tau_C<\tau_E$, where $\tau_C=\tau_S/[K_0(\infty)\,\mu_3(\infty)\,v(\tau_S)]^3$ denotes the coarsening time over which the supersaturation $\Delta(\tau)$ becomes zero, and $Q_0(\approx 0.14)$ is determined by $\tau_E(Q_0)=\tau_C(Q_0)$. This has already been discussed in I. The others are as follows.

Case [2] $Q_0<Q<Q_1$ with $\tau_S<\tau_E<\tau_C$:

$$\begin{aligned}&[\mathrm{E}]\quad 1\leqslant\tau<\tau_S: && K_0=\sigma\Phi=0,\qquad |\langle\lambda\rangle|\sim\langle a\rangle\\ &[\mathrm{I}]\quad \begin{cases}[\mathrm{I_S}] & \tau_S\leqslant\tau<\tau_E: \\ [\mathrm{I_{SE}}] & \tau_E\leqslant\tau<\tau_C:\end{cases} && \begin{aligned}&K_0\sim|\langle\lambda\rangle|\sim\langle a\rangle^{-1}\gg\sigma\Phi\\ &K_0\sim\sigma\Phi\gg|\langle\lambda\rangle|\sim\langle a\rangle^{-1}\end{aligned}\\ &[\mathrm{C}]\quad \tau_C\leqslant\tau: && K_0\sim\sigma\Phi\sim\tau^0\gg|\langle\lambda\rangle|\sim\langle a\rangle^{-1}\end{aligned}$$

Case [3] $Q_1 < Q$ with $\tau_E < \tau_S < \tau_C$:

$$
\begin{aligned}
&[\mathrm{E}] \quad 1 \leqslant \tau < \tau_E: && K_0 = \sigma\Phi = 0, \qquad |\langle\lambda\rangle| \sim \langle a\rangle \\
&[\mathrm{I}] \quad \begin{cases} [\mathrm{I_E}] & \tau_E \leqslant \tau < \tau_S: \\ [\mathrm{I_{SE}}] & \tau_S \leqslant \tau < \tau_C: \end{cases} && \begin{aligned} &K_0 \approx 0, \qquad \sigma\Phi \sim |\langle\lambda\rangle| \sim \langle a\rangle \\ &K_0 \sim \sigma\Phi \gg |\langle\lambda\rangle| \sim \langle a\rangle^{-1} \end{aligned} \\
&[\mathrm{C}] \quad \tau_C \leqslant \tau: && K_0 \sim \sigma\Phi \sim \tau^0 \gg |\langle\lambda\rangle| \sim \langle a\rangle^{-1}
\end{aligned}
$$

where $Q_1 (\approx 0.289)$ is determined by $\tau_E(Q_1) = \tau_S(Q_1)$. In Fig. 1 the volume fraction dependence of the characteristic times and stages is shown. Thus, we obtain the temporal power laws given by Eq. (4) and the time exponents which are shown in Fig. 1, where the time exponent $\eta_R = 4/9$ at stage [I] is predicted from the simulation. At stage [E] we have $\langle a\rangle(\tau)^2 = 2\tau$, and $v(\tau) = 1$ for all cases. At stage [C], we also find for all cases

$$\langle a\rangle(\tau)^3 = K\tau, \qquad v(\tau) = (\tau_S/\mu_3(\infty))(K\tau)^{-1} \tag{15}$$

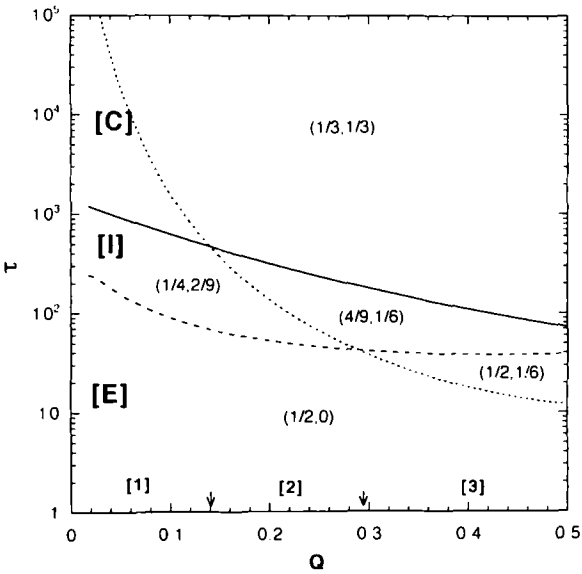

Fig. 1. The volume fraction dependence of the characteristic times. The dashed line, the dotted line, and the solid line indicate τ_S, τ_E, and τ_C, respectively. The numbers in the parentheses represent the time exponents (η_R, η_k). The arrows indicate the location of Q_0 and Q_1.

with the coarsening rate

$$K(Q) = K_0(\infty, Q) + \tau_S \sigma(\infty, Q)/\mu_3(\infty, Q) \tag{16}$$

where $\sigma(\infty, Q) \approx \mu_3(\infty)(16Q/\tau_S)^2$. Since Eq. (9) contains no adjustable parameters at stage [C], the distribution function $f(a, \tau)$ can also be obtained by solving it self-consistently under the boundary conditions $\mu_0(\tau) = \mu_1(\tau) = 1$. This will be discussed elsewhere.

3. NUMERICAL SIMULATION

In this section we discuss the numerical results obtained by simulating Eq. (7) directly. The encounter term, $(dR_i/d\tau)_E$, has the mechanism where when two droplets meet, the larger of them absorbs the smaller, conserving their total volume. This is simulated as follows. Whenever two droplets meet, we replace the volume of the larger droplet by their total volume and then move its position at their center of mass, while the smaller droplet is removed from the system. This procedure is done simultaneously. Since there will be a time for the larger droplet to form a spherical shape, absorbing the smaller one, a slight quantitative change may be expected at stage [I]. Since such a time scale is negligible compared to that of τ_C, however, the dynamics at stage [C] will not be influenced.

In the numerical simulation of Eq. (7), we have done the simulation 20 times to improve the statistics, each time with a different configuration of the droplets. The main procedure of the simulation is similar to that of Ref. 15. In the simulation the encounters are shown to be seldom when $Q < 0.1$. When $0.1 \leqslant Q < 0.2$, they are shown to occur sometimes, depending on what initial conditions one chooses. When $Q \geqslant 0.2$, they are shown always to occur whatever initial conditions one chooses. In Fig. 2 the log–log plot of the averaged droplet radius $\langle a \rangle(\tau)$ versus τ is shown for $Q = 0.2$ ($\bigcirc$), and 0.3 ($+$). For comparison, we also plot the analytical results without the encounter effect by the dashed line for $Q = 0.1$ and by the solid line for $Q = 0.2$. In Fig. 3 we show the histogram of the relative droplet size distribution function $F(\rho, \tau)$ for $Q = 0.2$ at $\tau = 10^5$. For comparison, we also show the analytical result obtained by solving Eq. (9) without the encounter term, $(\partial f/\partial \tau)_E$, for $Q = 0.2$ at $\tau = 10^5$ by the dashed line. Thus, the coagulation effect is turned out to broaden and flatten the relative droplet size distribution function. In Fig. 4 the coarsening rate $K(\tau)$ is plotted versus Q at $\tau = 10^5$. The analytical result obtained by neglecting the encounter effect is also shown by the solid line at $\tau = 10^5$ for comparison.

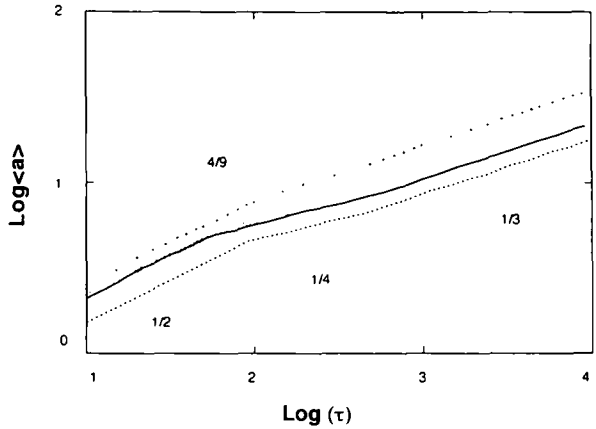

Fig. 2. A log–log plot of the average droplet radius versus time. Shown are the simulation data for $Q = 0.2$ (○) and $Q = 0.3$ (+). The dashed line and the solid line represent the theoretical results without the encounter effect for $Q = 0.1$ and 0.2, respectively.

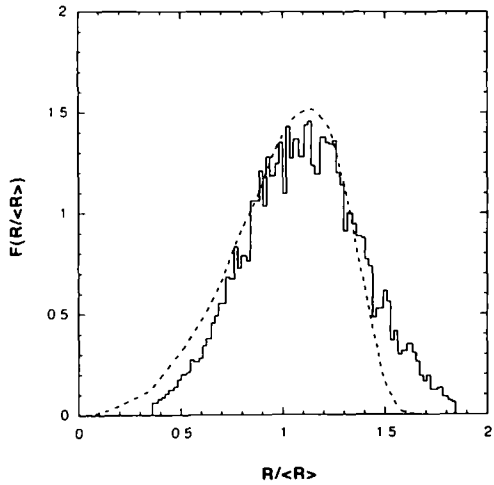

Fig. 3. The relative-droplet-size distribution function versus the relative droplet radius for $Q = 0.2$ at $\tau = 10^5$. The histogram indicates the result of the simulation with the encounter effect, and the dashed line the analytical result without it.

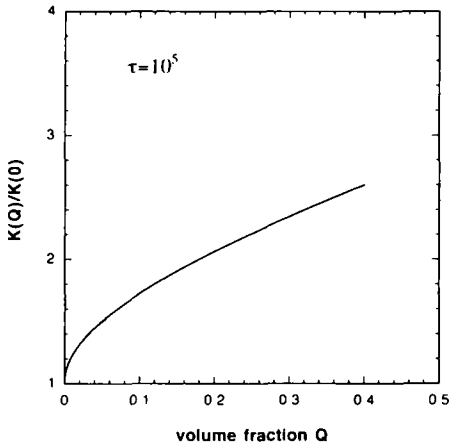

Fig. 4. The normalized coarsening rate as a function of volume fraction at $\tau = 10^5$. Circles indicate the result of the simulation, and the solid line the theoretical result without the encounter effect.

4. CONCLUSION

We have discussed the effect of a high-volume fraction on the dynamics of phase separations and shown that the coagulation effect strongly influences the growth kinetics qualitatively and quantitatively at stage [I] for $Q > Q_0$, while it makes only a quantitative change at stage [C]. In addition to the coagulation effect, the spatial correlations among droplets also start to play an important role in phase separations at a high volume fraction. This will be discussed elsewhere.

REFERENCES

1. For reviews, see *Dynamics of Ordering Processes in Condensed Matter*, S. Komura and H. Furukawa, eds. (Plenum, New York, 1988).
2. C. M. Knobler and N. C. Wong, *J. Phys. Chem.* **85**:1972 (1981).
3. K. Osamura, H. Okuda, Y. Amemiya, and H. Hashizume, *Metall. Trans.* **19A**:1973 (1988).
4. M. Hennion, D. Ronzaud, and P. Guyot, *Acta Metall.* **30**:599 (1982).
5. S. Katano and M. Iizumi, *Phys. Rev. Lett.* **52**:835 (1984).
6. A. H. Krall, J. V. Sengers, and K. Hamano, *Phys. Rev. E* **48**:357 (1993).
7. J. Marro, J. L. Lebowitz, and M. H. Kalos, *Phys. Rev. Lett.* **43**:282 (1979).
8. J. L. Lebowitz, J. Marro, and M. H. Kalos, *Acta Metall.* **30**:297 (1982).
9. P. Fratzl, J. L. Lebowitz, J. Marro, and M. H. Kalos, *Acta Metall.* **31**:1849 (1983).
10. K. Binder and D. Stauffer, *Phys. Rev. Lett.* **33**:1006 (1974).

11. K. Binder, *Phys. Rev. B* **15**:4425 (1977).
12. H. Furukawa, *Phys. Rev. Lett.* **43**:136 (1979).
13. J. S. Langer and A. J. Schwartz, *Phys. Rev. A* **21**:948 (1980).
14. J. D. Gunton, M. San Miguel, and P. S. Sahni, in *Phase Transitions and Critical Phenomena, Vol. 8*, C. Dome and J. L. Lebowitz, eds. (Academic, New York, 1983).
15. M. Tokuyama and Y. Enomoto, *Phys. Rev. E* **47**:1156 (1993). This is referred to as I.
16. M. Tokuyama and Y. Enomoto, *Phys. Rev. Lett.* **69**:312 (1992).
17. M. Tokuyama and Y. Enomoto, *Physica A* **204**:673 (1994).
18. I. M. Lifshitz and V. V. Slyozov, *J. Phys. Chem. Solids* **19**:35 (1961).